

Dynamic polarization and energy dissipation for charged particles moving in magnetized two-component plasmas

Zhang-Hu Hu, Yuan-Hong Song, and You-Nian Wang*

School of Physics and Optoelectronic Technology, Dalian University of Technology, Dalian 116024, People's Republic of China
(Received 23 August 2008; revised manuscript received 25 November 2008; published 9 January 2009)

Energy losses of test particles in magnetized two-component plasmas are investigated within the framework of the linearized Vlasov-Poisson theory, taking into account the dynamic polarization effects of both the plasma ions and electrons. General expressions of the potential and stopping power are obtained and calculations are performed for protons in a magnetized hydrogen plasma. The influences of the magnetic field, the angle between the proton velocity and magnetic field, and certain plasma parameters on the stopping power are studied. Numerical results show that for low particle velocities and strong magnetic field the dynamic polarization effects of the plasma ions become obvious and contribute mainly to the stopping power.

DOI: [10.1103/PhysRevE.79.016405](https://doi.org/10.1103/PhysRevE.79.016405)

PACS number(s): 52.40.Mj, 34.50.Bw, 52.25.Xz

I. INTRODUCTION

The energy loss of charged particles in plasmas have been an interesting topic, which is motivated by some applications, such as the inertial confinement fusion (ICF) driven by ion beams [1–5], and the neutral beam injection (NBI) [6–10] in the magnetically confined fusion plasmas. Especially, it has been proven that the NBI is a highly successful means of plasma heating, in which fast injected neutral particles are converted into fast ions within the plasma after impact ionizations and charge exchanges, and the fast ions slow down by transferring their energy and momentum to the plasma.

Usually, two main approaches, the dielectric theory and the binary collision approximation, are adopted in the investigations of the energy loss of charged particles in plasmas [11,12]. The basic assumption of the dielectric theory is that, being considered as a perturbation of the target plasma, the charged particles lose their energy by polarizing the surrounding plasma during the interaction. In this formulation, the linearized Vlasov-Poisson equations are usually employed to investigate the plasma polarization and the energy loss of the test particles in target plasma, which has been described as a Maxwellian plasma. The binary collision approximation, on the other hand, assumes that the stopping takes place in successive binary collisions between the charged particles and plasma particles. These two approaches above are only valid in the regimes where the plasma is close to ideal and the coupling between the test particle and the plasma target is weak. Besides, computer simulation methods, such as PIC and dynamic simulation, may be used to describe the strong-coupled interactions of the test particle with the plasma targets [11].

During the past decades, a number of theoretical calculation have been presented within theoretical framework of both the dielectric theory and the binary collision approximation [4,13–23]. Earlier, energy losses of charged particles have been investigated in plasmas without external magnetic field [4,13–15,17]. The maximum of the stopping power was

observed near the thermal velocity of the plasma electron, and the most important property of the stopping power at small velocities is the well-known linear velocity dependence theory provided that the plasma density is not too high [4,17]. It was found that the stopping is enhanced with the increase of the plasma density, while it is reduced as the temperature increases [17].

For the magnetic confinement fusion and electron cooling process, the magnetic field would play an important role in the stopping power [16,18–23]. An adequate analytical model for the stopping power in the case of extreme magnetization was presented [18,20], in which the “friction law” $S \propto u^2$ (where S is the energy loss rate and u is the particle velocity) is obtained in contrast to the linear velocity dependences without magnetic fields. In the subsequent work [23], the stopping power is calculated for arbitrary angles between the particle velocity and magnetic field, and a strong decrease of the energy loss has been noticed as the angle varies from 0 to $\pi/2$. In Ref. [21], the authors concentrated on the quantum mechanical treatment of the energy loss in magnetized plasma, in which analytical results were derived for the limit of high and low particle velocities, and the existence of the magnetic field is responsible for the reduction of the stopping power at high particle velocities, while enhancing the stopping power at low particle velocities.

However, to our knowledge, most of the theoretical studies on energy loss in magnetized plasmas have made the common assumption that the test particle travels in the electron plasmas with fixed ion background. And this assumption is justified if the ratio between the test particle velocity and plasma electron thermal velocity $u/v_{Te} > (m_e/m_i)^{1/3}$ (where m_e is the mass of the electron and m_i is the mass of the ion) as discussed in Ref. [15]. In this case, the dynamic polarization of ions and their effects on stopping charged particles could be neglected. Actually, without an external magnetic field, the ions in plasmas give an appreciably peaklike contribution to the stopping power only for particles with small velocities [4], and this kind of contribution is relatively small for big mass differences between electrons and ions [24]. However, in some applications, such as confined fusion, the effects of ion stopping have been found to be important [5]. In neutral beam injection experiments, the fractions of the

*ynwang@dlut.edu.cn

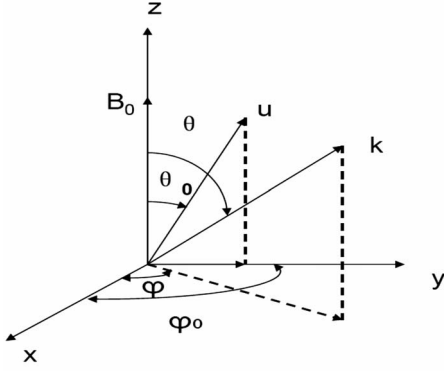


FIG. 1. Geometry of the vectors involved in this paper.

total beam energy that have gone to electrons and to ions are important quantities, which can describe the slowing-down process of the neutral beam [6,8]. As indicated in Ref. [8], for the beam energy higher than a critical energy W_c , the energy of the beam is lost predominantly to electrons. As the beam energy approaches W_c , energy loss to ions becomes important. Thus, one expects that for low particle velocity, the dynamic polarization of ions may exert a considerable influence on the stopping power. And the case under a strong magnetic field is also our concern.

In this work, a linearized dielectric theory is put forward to calculate the potential and energy loss of charged particles in magnetized two-component plasmas. The influences of magnetic field, the angles between the particle velocity and magnetic field, and the plasma parameters on the energy loss are taken into account. We focus our attention on the stopping power in the regions of low particle velocity and in the presence of the magnetic field, trying to reveal the importance of the dynamic polarization effects of ions and their contribution to the charged particle's energy loss. The paper is organized as follows. In Sec. II, the linearized Vlasov-Poisson equations are solved by means of Fourier analysis, obtaining a general form for the induced potential. In Sec. III, numerical results are discussed to analyze the stopping power of magnetized two-component plasmas. Finally, we give a short summary in Sec. IV.

II. INDUCED POTENTIAL

Consider a Cartesian coordinate system with $\mathbf{r}=\{x, y, z\}$ in Fig. 1, which is immersed in a large volume of magnetized plasma with density n_0 . The magnetic field \mathbf{B}_0 applied in the plasma is homogeneous and directed along the z axis. We shall use the subscripts $\sigma=e$ for plasma electrons and $\sigma=i$ for plasma ions. Now a charged particle with charge Z_1e and velocity \mathbf{u} moves in the magnetized plasma at an angle θ_0 with respect to the magnetic field \mathbf{B}_0 . The test particle is considered as a point charge and the space-charge density associated with it is $\rho_{ext}(\mathbf{r}, t)=Z_1e\delta(\mathbf{r}-\mathbf{u}t)$.

The linearized Vlasov equation of the two-component plasma may be written as

$$\frac{\partial f_{\sigma 1}}{\partial t} + \mathbf{v} \cdot \frac{\partial f_{\sigma 1}}{\partial \mathbf{r}} + \omega_{c\sigma}[\mathbf{v} \times \mathbf{b}] \cdot \frac{\partial f_{\sigma 1}}{\partial \mathbf{v}} = \frac{q_{\sigma}}{m_{\sigma}} \frac{\partial \phi}{\partial \mathbf{r}} \cdot \frac{\partial f_{\sigma 0}}{\partial \mathbf{v}}, \quad (1)$$

where $f_{\sigma}=f_{\sigma 0}+f_{\sigma 1}$; $f_{\sigma 1}$ is the first order perturbation of f_{σ} . And, the self-consistent electrostatic potential ϕ is determined by Poisson's equation

$$\epsilon_0 \nabla^2 \phi = -\rho_{ext}(\mathbf{r}, t) - \sum_{\sigma} q_{\sigma} \int d\mathbf{v} f_{\sigma 1}(\mathbf{r}, \mathbf{v}, t), \quad (2)$$

where \mathbf{b} is the unit vector parallel to \mathbf{B}_0 , q_{σ}, m_{σ} and $\omega_{c\sigma}=q_{\sigma}B_0/m_{\sigma}$ are the charge, mass, and cyclotron frequency of σ species, respectively. We denote the unperturbed distribution function of σ species as $f_{\sigma 0}$, which is taken uniform and Maxwellian,

$$f_{\sigma 0}(\mathbf{v}) = \frac{n_{\sigma 0}}{(2\pi v_{T\sigma}^2)^{3/2}} \exp\left(-\frac{v^2}{2v_{T\sigma}^2}\right), \quad (3)$$

with $v_{T\sigma}=\sqrt{k_B T_{\sigma}/m_{\sigma}}$ the thermal speed. Here, $T_{\sigma}, n_{\sigma 0}$ are the temperature and the unperturbed density of the σ species, respectively. For simplicity, we shall assume $n_{e0}=n_{i0}=n_0$. In Eq. (3), the temperatures of the electrons and the ions may be different, with each species described by its own Maxwellian distribution.

By means of the space-time Fourier transform

$$f_{\sigma 1}(\mathbf{r}, \mathbf{v}, t) = \int \int \frac{d\mathbf{k} d\omega}{(2\pi)^4} f_{\sigma 1}(\mathbf{k}, \mathbf{v}, \omega) e^{i\mathbf{k}\cdot(\mathbf{r}-\mathbf{u}t)}, \quad (4)$$

$$\mathbf{E}(\mathbf{r}, t) = \int \int \frac{d\mathbf{k} d\omega}{(2\pi)^4} \mathbf{E}(\mathbf{k}, \omega) e^{i\mathbf{k}\cdot(\mathbf{r}-\mathbf{u}t)}, \quad (5)$$

Eqs. (1) and (2) can be solved and the expression of the potential can be obtained by integrating along the unperturbed trajectory,

$$\phi(\mathbf{r}, t) = \frac{Z_1 e}{\epsilon_0 (2\pi)^3} \int d\mathbf{k} \frac{\exp[i\mathbf{k}\cdot(\mathbf{r}-\mathbf{u}t)]}{k^2 \epsilon(\mathbf{k}, \mathbf{k}\cdot\mathbf{u})}. \quad (6)$$

Here, $\epsilon(\mathbf{k}, \omega)$ is the dielectric function of the homogeneous two-component plasma, which has been given by Ichimaru [25], and could be written in the form as

$$\epsilon(\mathbf{k}, \omega) = 1 + \sum_{\sigma} \frac{k_{\sigma}^2}{k^2} \left\{ 1 + \sum_n \frac{\omega}{\omega - n\omega_{c\sigma}} \times \left[W\left(\frac{\omega - n\omega_{c\sigma}}{|k_{\parallel}|(T_{\sigma}/m_{\sigma})^{1/2}}\right) - 1 \right] \Lambda_n(\lambda_{\sigma}) \right\}, \quad (7)$$

where $k_{\sigma}=(n_0 e^2/\epsilon_0 T_{\sigma})^{1/2}$, W is the plasma dispersion function

$$W(Z) = 1 - Z \exp(-Z^2/2) \int_0^Z dy \exp(y^2/2) + i(\pi/2)^{1/2} Z \exp(-Z^2/2), \quad (8)$$

$\Lambda_n(\lambda_{\sigma})=I_n(\lambda_{\sigma})\exp(-\lambda_{\sigma})$, $\lambda_{\sigma}=k_{\perp}^2 T_{\sigma}/m_{\sigma} \omega_{c\sigma}^2$, and I_n is the modified Bessel function of the n th order. The symbols \parallel and \perp denote the components of the vector \mathbf{k} parallel or perpendicular to the external magnetic field, respectively. Also, the

dielectric function of a homogeneous two-component plasma without external magnetic field can be given as [25]

$$\varepsilon(\mathbf{k}, \omega) = 1 + \sum_{\sigma} \frac{k_{\sigma}^2}{k^2} W\left(\frac{\omega}{k(T_{\sigma}/m_{\sigma})^{1/2}}\right). \quad (9)$$

In general, the potential can be separated into two parts, viz.,

$$\phi(\mathbf{r}, t) = \frac{Z_1 e}{4\pi\epsilon_0|\mathbf{r} - \mathbf{u}t|} + \phi_{ind}(\mathbf{r}, t), \quad (10)$$

where the first part is the bare Coulomb potential of the test particle and the second part is the induced potential caused by the test particle. In the cylindrical coordinates (see corresponding geometry in Fig. 1), the induced potential can be written as

$$\phi_{ind}(\mathbf{r}, t) = \frac{Z_1 e}{\epsilon_0(2\pi)^2} \int_0^{\infty} k_{\perp} dk_{\perp} \int_{-\infty}^{+\infty} dk_{\parallel} \frac{\Pi(k_{\parallel}, k_{\perp}, \mathbf{k} \cdot \mathbf{u}, \mathbf{r}, t)}{k_{\parallel}^2 + k_{\perp}^2}, \quad (11)$$

where

$$\begin{aligned} \Pi(k_{\parallel}, k_{\perp}, \mathbf{k} \cdot \mathbf{u}, \mathbf{r}, t) = & \text{Re}[\varepsilon^{-1}(k_{\parallel}, k_{\perp}, \mathbf{k} \cdot \mathbf{u}) - 1] \cos[\mathbf{k} \cdot (\mathbf{r} - \mathbf{u}t)] \\ & + \text{Im}[-\varepsilon^{-1}(k_{\parallel}, k_{\perp}, \mathbf{k} \cdot \mathbf{u}) - 1] \\ & \times \sin[\mathbf{k} \cdot (\mathbf{r} - \mathbf{u}t)]. \end{aligned} \quad (12)$$

Here, we take $\mathbf{k} \cdot \mathbf{u} = k_{\parallel} u_{\parallel} + k_{\perp} u_{\perp}$, and $\varepsilon(k_{\parallel}, k_{\perp}, \omega) = \varepsilon_r + i\varepsilon_i$ in terms of its real part ε_r and imaginary part ε_i .

In this paper, we only take into account a hydrogen plasma and the main parameters used here are closed to the parameters in fusion plasmas. The base values of the parameters are as follows, unless otherwise indicated: the plasma density, $n_0 = 10^{18} \text{ m}^{-3}$; the unperturbed densities of plasma electrons and plasma ions, $n_{e0} = n_{i0} = 10^{18} \text{ m}^{-3}$; the ion temperature, $T_i = 500 \text{ eV}$; and the electron temperature, $T_e = 1 \text{ keV}$. We have the ion charge $q_i = e$ and the mass ratio $m_i/m_e = 1836$ for a hydrogen plasma. Besides, we take the following dimensionless quantities as $k_{\parallel} \rightarrow k_{\parallel} \lambda_{De}$, $k_{\perp} \rightarrow k_{\perp} \lambda_{De}$, $k \rightarrow k \lambda_{De}$, $\omega \rightarrow \omega/\omega_{pe}$, $u \rightarrow u/v_{Ti}$, and $\omega_{c\sigma} \rightarrow \omega_{c\sigma}/\omega_{p\sigma}$, where $\lambda_{De} = \sqrt{\epsilon_0 T_e / n_0 e^2}$ is the Debye length of the electrons and $\omega_{p\sigma} = \sqrt{n_0 q_{\sigma}^2 / m_{\sigma} \epsilon_0}$ is the plasma frequency of the σ species. In addition, a proton with fixed charge $Z_1 e = e$ is taken as the test particle.

We first plot (a) the real part $\varepsilon_r(k_{\parallel}, k_{\perp}, \omega)$ and (b) the imaginary part $\varepsilon_i(k_{\parallel}, k_{\perp}, \omega)$ of the dielectric function as a function of ω in the units of $\omega_{pe} = \sqrt{n_0 e^2 / \epsilon_0 m_e}$ for various values of magnetic field in Fig. 2. Here, $k_{\parallel} \lambda_{De} = 1/2$, $k_{\perp} \lambda_{De} = 1/2$ are kept fixed. One can see that $\varepsilon_r(k_{\parallel}, k_{\perp}, \omega)$ decreases obviously with the increasing magnetic field. Meanwhile, the magnetic field enhances $\varepsilon_i(k_{\parallel}, k_{\perp}, \omega)$ only in the low frequency region and shows almost no effects in the high frequency regions. In particular, one can see from Figs. 2(a) and 2(b) that both $\varepsilon_r(k_{\parallel}, k_{\perp}, \omega)$ and $\varepsilon_i(k_{\parallel}, k_{\perp}, \omega)$ have two minimum or maximum values near the frequencies $\omega_{pi}/2$ and $\omega_{pe}/2$, corresponding to collective excitations of the ions and electrons.

In Fig. 3, we show the dependences of the potential ϕ on the dimensionless distance $(z - z_d)/\lambda_{De}$ for protons traveling parallel to the magnetic field, with Figs. 3(a) and 3(b) shown

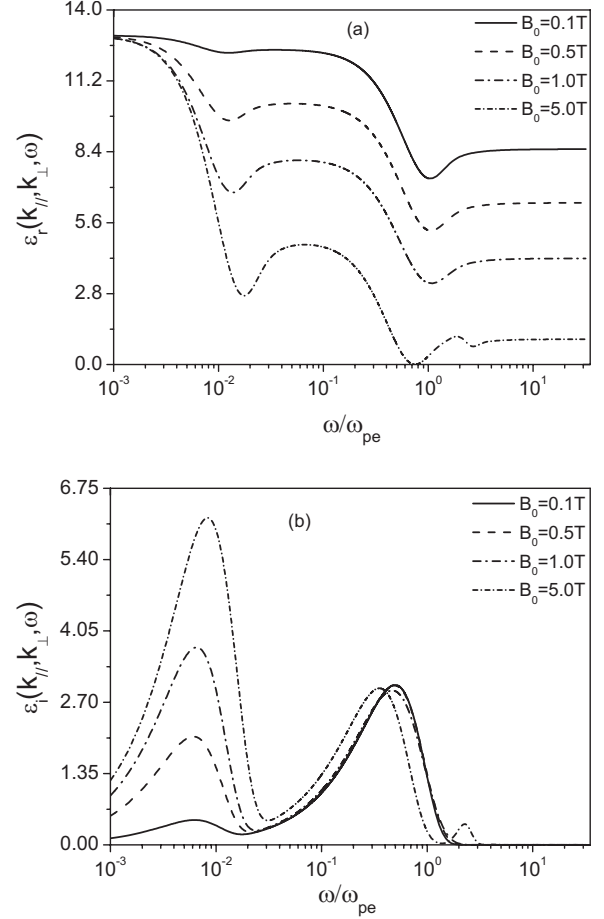


FIG. 2. The real part $\varepsilon_r(k_{\parallel}, k_{\perp}, \omega)$ (a) and imaginary part $\varepsilon_i(k_{\parallel}, k_{\perp}, \omega)$ (b) of the dielectric function vs ω for various values of the magnetic field. Here, $k_{\parallel} \lambda_{De} = 1/2$, $k_{\perp} \lambda_{De} = 1/2$.

for different values of magnetic field and particle velocities, respectively. One may notice from Fig. 3(a) that, for the case of the particle velocity $u/v_{Ti} = 3.01$, as the magnetic field increases, the magnitude of the wake potential increases significantly due to the stronger polarization of the medium. Also as shown in Fig. 3(b), as the velocity of the particle increases, the wake potential shows a longer oscillation tail behind the test particle, similar to the case without the magnetic field.

III. STOPPING POWER

The stopping power of the test particle S is defined as the energy loss of the particle per unit length due to the plasma polarization. From Eq. (11) it is straightforward to calculate the induced electric field $\mathbf{E}_{ind} = -\nabla \phi_{ind}$, and the stopping force acting on the particle. Thus, the stopping power of the particle becomes

$$\begin{aligned} S &= Z_1 e \frac{\mathbf{u}}{u} \cdot \left. \frac{\partial \phi_{ind}}{\partial \mathbf{r}} \right|_{\mathbf{r}=\mathbf{u}t} \\ &= \frac{(Z_1 e)^2}{\epsilon_0 (2\pi)^3} \int \frac{d^3 k \cdot \mathbf{u}}{k^2 u} \text{Im} \left(\frac{-1}{\varepsilon(\mathbf{k}, \mathbf{k} \cdot \mathbf{u})} \right). \end{aligned} \quad (13)$$

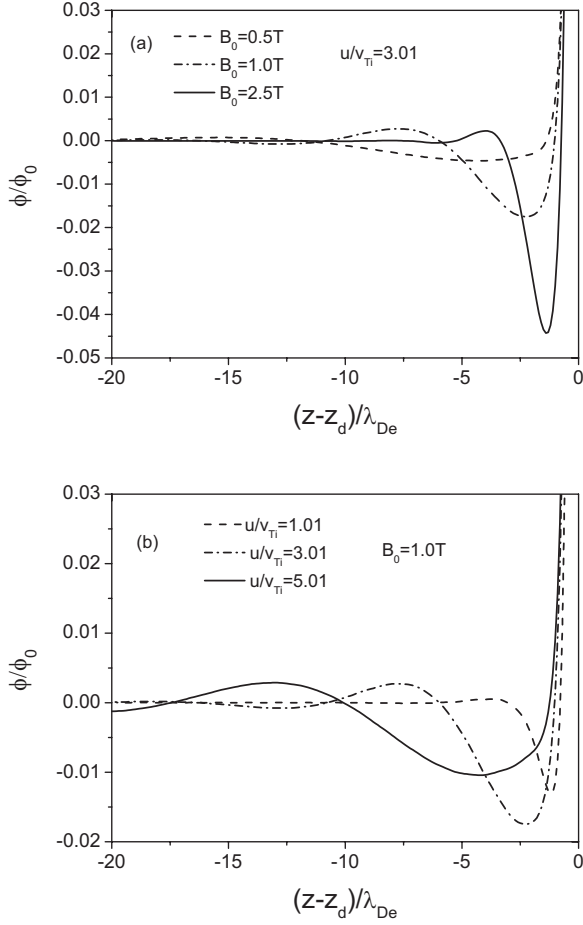


FIG. 3. The potential ϕ along the z axis as a function of the distance $(z-z_d)/\lambda_{De}$ for (a) different values of the magnetic field with fixed particle velocity and (b) different values of the particle velocity relative to v_{Ti} with a fixed magnetic field. Here, $\theta_0=0$ for the case of $\mathbf{u}\parallel\mathbf{B}_0$, $z_d=ut$ is the position of the test particle, and $\phi_0=e/(\epsilon_0\lambda_{De})$.

To show more clearly the contribution of plasma ions and electrons to the stopping power, an approximation [12,26] is introduced here in which the effective, dynamic particle-electron and particle-ion interactions are replaced by the statically screened interactions. In this approximation the stopping power reads as

$$S = \frac{(Z_1 e)^2}{\epsilon_0 (2\pi)^3} \int d^3k \frac{\mathbf{k} \cdot \mathbf{u}}{u} \frac{k^2}{(k^2 + \beta^2)^2} \text{Im} \epsilon(\mathbf{k}, \mathbf{k} \cdot \mathbf{u}). \quad (14)$$

Here the parameter $\beta = (\lambda_{De}^{-2} + \lambda_{Di}^{-2})^{1/2}$ describes the collective static shielding of the test particle, and the imaginary part of the dielectric function takes the form as

$$\begin{aligned} \text{Im} \epsilon(\mathbf{k}, \omega) &= \sum_{\sigma} \frac{\sqrt{\pi} \omega k_{\sigma}^2}{k^2 |\mathbf{k}_{\parallel}| (T_{\sigma}/m_{\sigma})^{1/2}} \sum_n \Lambda_n(\lambda_{\sigma}) \\ &\quad \times \exp \left[- \left(\frac{\omega - n \omega_{c\sigma}}{|\mathbf{k}_{\parallel}| (T_{\sigma}/m_{\sigma})^{1/2}} \right)^2 \right] \\ &\equiv \text{Im} \epsilon_e(\mathbf{k}, \omega) + \text{Im} \epsilon_i(\mathbf{k}, \omega). \end{aligned}$$

The simplified stopping power S in Eq. (14), which neglects

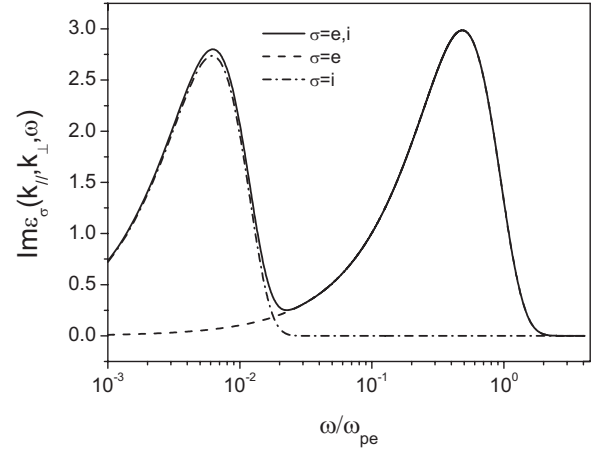


FIG. 4. The ion ($\sigma=i$) and electron ($\sigma=e$) contributions to the imaginary part of the dielectric function. Here, $k_{\parallel}\lambda_{De}=1/2$, $k_{\perp}\lambda_{De}=1/2$, and the magnetic field $B_0=1$ T.

the dynamic collective modes in the plasma [26], is mainly determined by the imaginary part of the dielectric function. In order to show the ion and electron contribution to the stopping power, we plot $\text{Im} \epsilon(\mathbf{k}, \omega)$, $\text{Im} \epsilon_e(\mathbf{k}, \omega)$, and $\text{Im} \epsilon_i(\mathbf{k}, \omega)$ as a function of ω in Fig. 4. Here $k_{\parallel}\lambda_{De}=1/2$, $k_{\perp}\lambda_{De}=1/2$, $B_0=1$ T, and the other parameters are the same as those in Figs. 2 and 3. It is clearly seen that the ion polarization contributes mainly to the part located at low frequencies, while a reversed behavior can be observed for the electrons excitation. Thus, the stopping power in magnetized two-component plasmas might be calculated approximately by first taking into account only the ions dynamically at the low frequency part, and then only the electrons at the high frequency part, and finally, adding the two contributions together, as $S \sim S_e + S_i$. This treatment of the stopping power in magnetized two-component plasmas is similar to that without a magnetic field [4].

In Fig. 5, we show the influence of the magnetic field on the stopping power as a function of the proton velocity u/v_{Ti} , with the angle $\theta_0 = \pi/6$, and the other parameters the same as those in Figs. 2 and 3. Both Figs. 5(a) and 5(b) show that the stopping power has two maximum values, with one located near the thermal velocity of plasma ions v_{Ti} corresponding to the collective excitation of plasma ions, and with the other one near the thermal velocity of plasma electrons v_{Te} with respect to the collective excitation of plasma electrons. From the low particle velocity region $u/v_{Te} < 1$, it is easily seen that the test proton is exposed to more stopping significantly from the plasma ions with the increasing magnetic field. This is also indicated in Fig. 2(b), in which the imaginary part of the dielectric function at low frequencies increases significantly with the increase of the magnetic field. However, for particles with high velocities $u/v_{Te} > 1$, we notice that the increase of the magnetic field also enhances the stopping power for the case of the weak magnetic field $\omega_{ce}/\omega_{pe} < 1$, but only makes the electron stopping profiles shift slightly to the lower velocity region for stronger magnetic field $\omega_{ce}/\omega_{pe} > 1$. As we all know, under the influence of a strong magnetic field, the motion of the electrons transverse to the magnetic field becomes increasingly restricted. In this case,

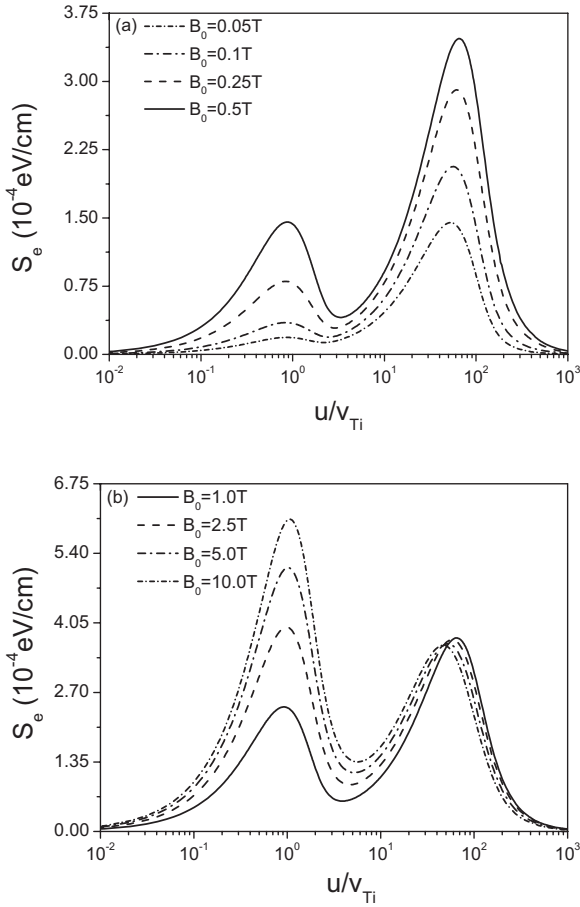


FIG. 5. Influence of (a) weak magnetic field with $\omega_{ce}/\omega_{pe} < 1$, (b) strong magnetic field with $\omega_{ce}/\omega_{pe} > 1$ on the stopping power of protons as a function of the proton velocity u . Here, the plasma density $n_0=10^{18} \text{ m}^{-3}$, the electron temperature $T_e=1 \text{ keV}$, the ion temperature $T_i=500 \text{ eV}$, and $\theta_0=\pi/6$.

the electrons cannot respond thoroughly to the disturbance from the intrusive ions. On the contrary, the dynamic polarization of the plasma ions becomes more active, leading to the increasing energy transfer from the test ion to the plasma ions. These results suggest that in the presence of a weak magnetic field, the energy losses of the incident ions with low velocities is smaller than those with high velocities, while under the strong magnetic field, the ions with low velocities play an important role in the energy exchange with plasmas.

We further show the locations of the two maximum values in the stopping power for different magnetic fields in Fig. 6. Here S_{max1} and S_{max2} represent the maximum values at relatively low and high velocities, respectively. And the other parameters are same as those in Fig. 5. The locations of the two maximum values are indeed near the thermal velocities of plasma ions and electrons.

Figure 7 shows the influences of different angles $\theta_0=0, \pi/6, \pi/3$, and $\pi/2$ on the stopping power in plasmas with magnetic field $B_0=1 \text{ T}$. One can see from this figure that, as the angle θ_0 increases, both of the stopping power peaks move to a higher velocity region, indicating the incident ions with higher energy will experience more stopping. In addition,

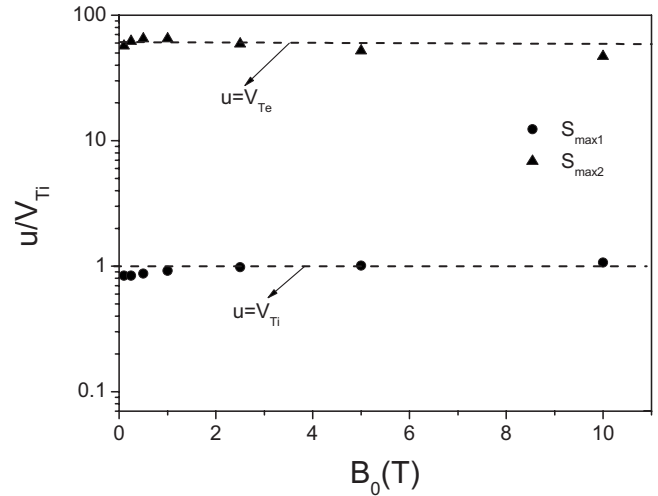


FIG. 6. The locations of the two maximum values of the stopping power for different magnetic fields. Here S_{max1} and S_{max2} represent the maximum values at relatively low and high velocities, respectively, and the other parameters are the same as those in Fig. 5.

tion, the two peak values decrease, showing less effects from the magnetic field, with the increasing angle θ_0 between the magnetic field and the velocity of the test ion.

We further plot in Fig. 8 the stopping power as a function of the velocity u for different plasma parameters, with only the angle $\theta_0=\pi/6$ and the magnetic field $B_0=1 \text{ T}$ kept fixed. Figure 8(a) shows that both the magnitude of ion stopping and electron stopping increase significantly with the increasing plasma density from $n_0=10^{18} \text{ m}^{-3}$ to $n_0=10^{19} \text{ m}^{-3}$, without any shifts of the peaks location. Figure 8(b) shows us the stopping power with several electron temperatures, in which the influences of the electron temperature on the ion stopping and on the electron stopping are different. The ion stopping increases slightly, while the electron stopping decreases significantly with the increasing electron temperature. In our opinion, the frequencies of collective modes associated with

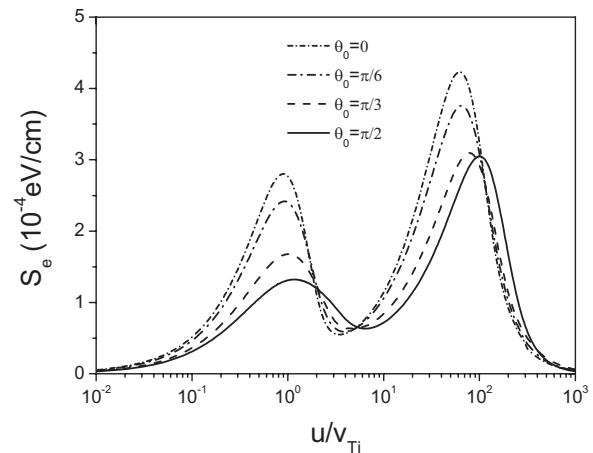


FIG. 7. Influence of angle θ_0 on the stopping power of protons as a function of the proton velocity u . Here, the plasma density $n_0=10^{18} \text{ m}^{-3}$, the electron temperature $T_e=1 \text{ keV}$, the ion temperature $T_i=500 \text{ eV}$, and the magnetic field $B_0=1 \text{ T}$.

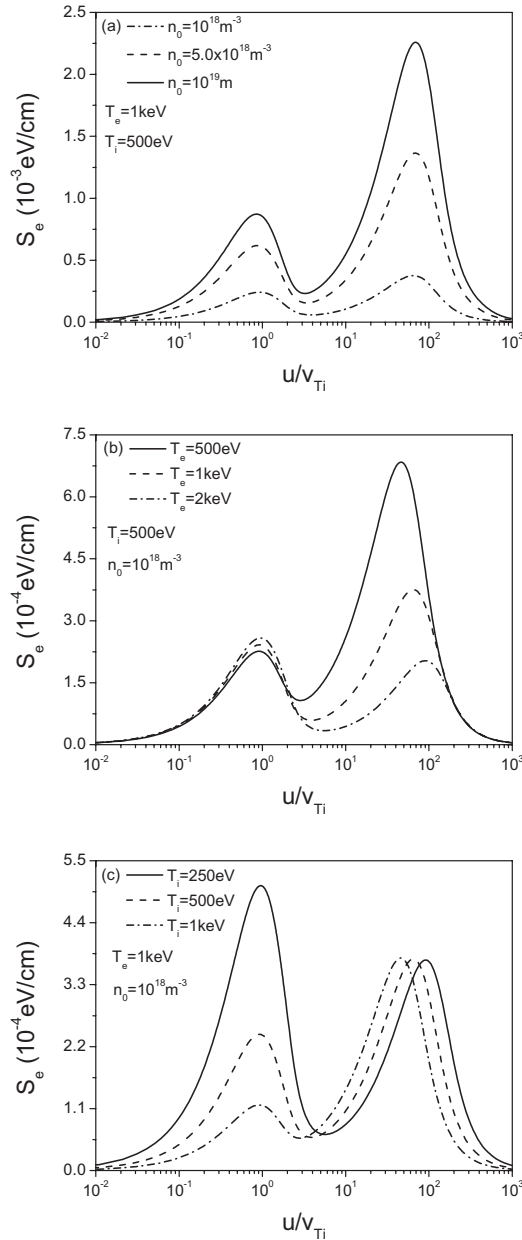


FIG. 8. Influence of (a) the plasma density n_0 , (b) the electron temperature T_e , and (c) the ion temperature T_i on the stopping power of protons as a function of the proton velocity u . Here, the magnetic field $B_0 = 1$ T and $\theta_0 = \pi/6$.

ions are so low that the mobile electrons can easily follow the motion of the ions and screen their electrostatic fields. So one can expect that different electron temperatures exert a

slight influence on the ion stopping. Also, the ion temperature can only affect the ion stopping, as indicated in Fig. 8(c), where the ion stopping decreases significantly with the increasing ion temperature. Note that in both Figs. 8(b) and 8(c) the ion stopping exceeds the electron stopping for $T_e/T_i \geq 4$ [see $T_i = 500$ eV, $T_e = 2$ keV in Fig. 8(b) and $T_e = 1$ keV, $T_i = 250$ eV in Fig. 8(c)]. So one can expect that for $T_e/T_i \geq 1$ the dynamic polarization effects of ions may become very obvious.

IV. SUMMARY

Based on the linearized Vlasov-Poisson theory, we have studied the energy losses of charged particles in magnetized two-component plasmas. Influences of the magnetic field, angle θ_0 formed by the magnetic field and the proton velocity, and certain plasma parameters on the stopping power of both the plasma ions and electrons are discussed. In particular, we have focused our attention on plasma ions polarization in the low particle velocity region and the influence of magnetic field on the stopping power.

Numerical results show that, under the influence of a strong magnetic field, the dynamic polarization effects of plasma ions become more obvious and the ion stopping contributes mainly to the energy losses of the incident particle with low velocity $u/v_{Te} < 1$. On the other hand, the plasma electrons stopping to the particle with high velocity $u/v_{Te} > 1$ becomes dominant in the presence of weak magnetic effects. We have also investigated the influence of angle θ_0 and some plasma parameters on the stopping power. It is noticed that, with the increase of angle θ_0 not only the peak values of both the ion and electron stopping powers decrease, but also the positions at which the peak values located move to a higher velocity region. Moreover, both the ion and electron stopping powers increase definitely with the increase of the plasma density, but show strong dependences only on their own temperature.

In this work, our results indicate that the ion stopping becomes important to the slowing-down process of the beam with a strong magnetic field applied in the plasma. We believe that the results obtained will provide a helpful reference to the experiments relative to fusion plasmas, such as heating by neutral beam injection. And, our further attention will concentrate on the collision and energy deposition process for the incident neutral beam with the plasma.

ACKNOWLEDGMENT

This work is supported by the National Basic Research Program of China (Grant No. 2008CB717801).

[1] D. Keefe, *Annu. Rev. Nucl. Part. Sci.* **32**, 391 (1982).
 [2] C. Deutsch, *Ann. Phys. (Paris)* **11**, 1 (1986).
 [3] R. C. Arnold and J. Meyer-ter-Vehn, *Rep. Prog. Phys.* **50**, 559 (1987).
 [4] T. Peter and J. Meyer-ter-Vehn, *Phys. Rev. A* **43**, 1998 (1991).

[5] C. K. Li and R. D. Petrasso, *Phys. Rev. Lett.* **70**, 3059 (1993).
 [6] T. H. Stix, *Plasma Phys.* **14**, 367 (1972).
 [7] S. L. Davis, V. Arunasalam, R. J. Hawryluk, M. Okabayashi, G. L. Schmidt, J. L. Schmidt, and S. Suckewer, *Phys. Fluids* **20**, 1571 (1977).

- [8] E. Speth, Rep. Prog. Phys. **52**, 57 (1989).
- [9] E. Thompson, D. Stork, H. P. L. de Esch, and the JET Team, Phys. Fluids B **5**, 2468 (1993).
- [10] T. Takahashi, T. Kato, and Y. Kondoh, Phys. Plasmas **11**, 3801 (2004).
- [11] G. Zwicknagel, C. Toepffer, and P.-G. Reinhard, Phys. Rep. **309**, 117 (1999).
- [12] H. B. Nersisyan, G. Zwicknagel, and C. Toepffer, Phys. Rev. E **67**, 026411 (2003).
- [13] J. Neufeld and R. H. Ritchie, Phys. Rev. **98**, 1632 (1955).
- [14] I. A. Akhiezer, Zh. Eksp. Teor. Fiz. **40**, 954 (1961); [Sov. Phys. JETP **13**, 667 (1961)].
- [15] S. T. Butler and M. J. Buckingham, Phys. Rev. **126**, 1 (1962).
- [16] R. M. May and N. F. Cramer, Phys. Fluids **13**, 1766 (1970).
- [17] L. de Ferrariis and N. R. Arista, Phys. Rev. A **29**, 2145 (1984).
- [18] H. B. Nersisyan, Phys. Rev. E **58**, 3686 (1998); H. B. Nersisyan and C. Deutsch, Phys. Lett. A **246**, 325 (1998).
- [19] H. B. Nersisyan, M. Walter and G. Zwicknagel, Phys. Rev. E **61**, 7022 (2000).
- [20] C. Cereceda, C. Deutsch, M. De Peretti, M. Sabatier, and H. B. Nersisyan, Phys. Plasmas **7**, 2884 (2000).
- [21] M. Steinberg and J. Ortner, Phys. Rev. E **63**, 046401 (2001).
- [22] H. B. Nersisyan, G. Zwicknagel, and C. Toepffer, Phys. Rev. E **67**, 026411 (2003).
- [23] C. Cereceda, M. De Peretti, and C. Deutsch, Phys. Plasmas **12**, 022102 (2005).
- [24] K. Morawetz and G. Ropke, Phys. Rev. E **54**, 4134 (1996).
- [25] S. Ichimaru, *Basic Principles of Plasma Physics: A Statistical Approach* (Benjamin, Reading, Mass., 1973), Secs. 3.4, 10.4 and 4.4.
- [26] M. Walter, G. Zwicknagel, and C. Toepffer, Eur. Phys. J. D **35**, 527 (2005).